Experimental Study For a Laminar Natural Convection Heat Transfer From an Isothermal Heated Square Plate With and Without Circular Hole

Asst. Prof. Dr. Ikhlase M. Fayed* & Asst. Lec. Wassan N. Matti**

ABSTRACT

An experimental investigation of natural convection heat transfer from an isothermal horizontal, vertical and inclined heated square flat plates with and without circular hole, were carried out in two cases, perforated plates without an impermeable adiabatic hole "open core" and perforated plates with an impermeable adiabatic hole "closed core" by adiabatic plug. The experiments covered the laminar region with a range of Rayleih number of ($1.11x10^6 \le Ra_{Lo} \le 4.39x10^6$), at Prandtle number (Pr=0.7). Practical experiments have been done with variable inclination angles from horizon ($\Phi=0^o,45^o,90^o,135^o$ and 180^o), facing upward ($0^o \le \Phi < 90^o$), and downward ($90^o \le \Phi < 180^o$). The results showed that the temperature gradient increases while the thermal boundary layer thickness decreases when Grashof number and perforation ratio (m) increase . The temperature gradient for inclined position facing upward is less than facing downward, while the thermal boundary layer thickness is greater. The temperature gradient decreases while the thermal boundary layer thickness increases for perforated plates with an adiabatic core as compared with perforated plates without an adiabatic core. The value of average Nusselt number increases with increasing perforation ratio, and Grashof number for all specimens with and without an adiabatic core, also increases by increase in inclination of plates approaching the higher value at vertical position ($\Phi=90^o$), then decreases with increasing inclination of plates till horizontal position ($\Phi=180^o$). The average Nusselt number values for perforated plates with an adiabatic core are lower than for perforated plates without an adiabatic core for all perforation ratios. Maximum heat transfer rate occurs at perforated plate with perforation ratio of (m=0.1) without adiabatic core for vertical position ($\Phi=90^o$), at a range of Grashof number ($1.576x10^6 \le Gr_{Lo} \le 6.292x10^6$), while the rate of heat transfer decreases with increasing perforation ratio for plates with and without adiabatic core for decrease in heat transfer rate area. The rate of heat transfer for perforated plates with circular hole is more than for perforated plates with square hole at the same perforation ratios (m=0.1,0.16,0.24 and 0.36). It found that the lack of core flow decreases the overall heat transfer rate by (6.477%) . There was a good agreement for the experimental present work results compared with other pervious results .

الخلاصة

يقدم البحث الحالي دراسة عملية لانتقال الحرارة بالحمل الحر من صفائح مربعة افقية وعمودية ومائلة عن الافق وذات ثقب دائري مسخنة بثبوت درجة الحرارة، لحالتي النماذج المثقبة بوجود سداد للثقب الدائري وعدم وجوده، ضمن منطقة الجريان الطباقي لرقم رالي ($1.11x10^6 \le Ra_{Lo} \le 4.39x10^6$)، عند رقم برانتدل Pr=0.7. اجريت التجارب العملية لمدى من زوايا الميل عن الافق ($\Phi=0^o,45^o,90^o,135^o\&180^o$) لوجه التسخين للأعلى وللأسفل. اظهرت النتائج ان انحدار درجات الحرارة يزداد فيما يقل سمك الطبقة المتاخمة الحرارية (δ) عند زيادة رقم كراشوف ونسبة التثقيب، فيكون انحدار درجات الحرارة للوضع المائل في حالة التسخين باتجاه الاعلى اقل من حالة التسخين باتجاه الاسفل بينما سمك الطبقة المتاخمة الحرارية اكبر، كما ان انحدار درجات الحرارة يقل بينما يزداد سمك الطبقة المتاخمة الحرارية للصفائح المثقبة بوجود السداد عن عدم وجوده . تزداد قيمة متوسط رقم نسلت بزيادة رقم كراشوف وبنسبة التثقيب (m) بوجود وعدم وجود السداد، وتزداد قيمة متوسط رقم نسلت مع ازدياد الميلان في حالة التسخين الى الاعلى الى ان تصل اعظم قيمة لها عند الوضع العمودي ($\Phi=90^o$) ثم تقل بزيادة زاوية الميلان في حالة التسخين الى الاسفل وصولا الى الوضع الافقي ($\Phi=180^o$). لجميع نسب التثقيب تكون قيم متوسط رقم نسلت اقل للصفائح المثقبة بوجود السداد عن الصفائح المثقبة بدون وجود السداد. اقصى قيمة لكمية الحرارة المنتقلة تكون للصفيحة المثقبة بنسبة التثقيب (m=0.1) بدون وجود السداد في حالة الوضع العمودي ($\Phi=90^o$) لمدى رقم كراشوف ($1.57x10^6 \le Gr_{Lo} \le 6.292x10^6$)، وتقل كمية الحرارة المنتقلة بزيادة نسبة التثقيب بسبب النقصان الحاصل في مساحة سطح التبادل الحراري الذي يؤدي الى الانخفاض في معدل انتقال الحرارة للصفائح المثقبة بوجود وعدم وجود السداد .إن كمية الحرارة المنتقلة للصفائح المثقبة بثقب دائري اكبر من كمية الحرارة المنتقلة للصفائح المثقبة بثقب مربع لنفس نسب التثقيب (m=0.1,0.16,0.24,0.36). وكانت كمية الحرارة اللابعدية (Q) للنماذج المثقبة بوجود السداد للثقب تقل عن كمية الحرارة اللابعدية (Q) بدون وجوده بنسبة (6.477%). هناك توافق جيد للنتائج العملية للبحث الحالي مع نتائج بحوث سابقة .

Key Words: **Natural Convection, Square Plate With and Without Circular Hole, Facing Upward and Downward.**

***Dept. of Mech. Eng., University of Technology, Baghdad-Iraq.**

INTRODUCTION

Decades ago have witnessed a great interest for the process of convection heat transfer from finite bodies such as (square surface) because of its wide spread application in many engineering and industrial applications, which include the heat flow from streaming radiant, cooling small electronic devices that have low power, air conditioning, warming systems in rooms, building walls, the natural convection enters in nuclear power applications for cooling objects surfaces that diffusion heat is generated in. It is also used in heat transfer resulting from chemical reactions, and in the environment, libratory devices, cooking, also natural convection can be found in engineering system such as heat exchange fin surfaces applications, electronic parts that have different shapes, electrical natural convection furnaces, heaters devices, and some load cell.

Natural Convection heat transfer from isothermal plates continues to be a topic of current research, and also a number of experimental and theoretical studies **[AL-Arabi & EL-Riedy (1976), Mustafa (2001), Aziz (2002), Robinson & Liburdy (1987) ,Pera &Gebhart (1973), Sahraoui et al. (1990)]** have been made in past to determine the natural convection heat transfer from heated isothermal plates hold in horizontal position, the convective flow situation is two dimensional and thus easier to study experimentally and theoretically. Two earliest studies **[Abd (2007)]** has been done theoretical study for a three-dimensional natural convection heat transfer from an isothermal horizontal , vertical and inclined heated square flat plates (with and without circle hole) which involved the numerical solution of the transient Navier-Stokes and energy equations by using Finite Different Method (F.D.M.), & **[Ali (2007)]** has been done experimental study for isothermal square flat plate (with and without square hole) with extension surface. The experiments covered the laminar region with a range of Rayleigh number of order of 10^6, and included the manufacturing of four square models of aluminum (10cm) length, (1cm) thickness and perforation ratio (m=0.0,0.04,0.16&0.36) respectively with heater for each model for inclined position for square plate of constant temperature. Table (1) shows the results of previous studies.

The present experimental investigation aims to study the natural convection heat transfer from isothermal heated square plate, with and without circular hole, for different perforation ratio in two cases, perforator plates with and without adiabatic circular hole, and the effect of different inclination angle from horizon ($\Phi=0^o$, 45^o, 90^o, 135^o and 180^o), facing upward and downward, different ranges of Grashof number ($1.576\times10^6 \leq Gr \leq 6.292\times10^6$), then analysis the results to develop mathematical relationships that rely on the accounts (arithmetic) of natural convection taking into consideration the effect of inclination angles (Φ), perforation ratio (m) and heating levels.

EXPERIMENTAL APPARATUS

Manufacturing four specimens used as a heat exchange surfaces are made of aluminum sheets, having square shape with length and thickness (100mm and 10mm) respectively. A basic dimensions of the specimens are given in Table (2). The first specimen is a square shape, but the other specimens are perforated with circular hole at different perforated area (m=0.0,0.1,0.24 and 0.5) as shown in Figure (1). In order to measure the surface temperature homogeneity of the specimen, a copper-constantan type (T) thermocouples, embedded from the heated surface. The four specimens were drilled with a number of holes with diameter (2mm) and depth (9mm) from the bottom. The holes were distributed radialy with a pitch angle of 45^o and radii (36, 40 and 45mm) for the specimens designated as 2-nd, 3-rd, and 4-th respectively. To heat up the heat exchange surfaces (specimens), an electric heaters are manufactured from nickrom (nickel-chromium alloy). In order to study the natural heat transfer for inclination angles from horizon ranging from (0^o to 180^o), the wooden extending surface which contains the heat exchange surfaces (specimens) have been installed on the apparatus bracket. It can be moved by moving

joints fitted between the extending surface and apparatus bracket, with the inclination angle could be controlled through the manual metal protractor, as shown in Figure (2).
A uniform temperature on the surface of the model was achieved by adjusting the electrical input power to the heating element . The specimen and heating element assembly were installed for the purpose of conducting the study with its own heater together with the wooden extending surface to ensure parallel flow at the specimen edges. The surface heat exchange (specimen) was isolated together with the heater from all sides, except the upper surface to reduce thermal losses. To minimize side effects of air currents room temperature in the process of natural heat transfer from heat exchange surfaces, the apparatus was placed in a room with dimensions (4m x 2m x 3m). In order to study the heat transfer by natural convection from the surface of a specimen, the surface air temperatures were measured by a thermocouple, which was installed in a holder with shape (∩), to move the holder on the specimen surface in three dimensions (x, y, z), it is connected with three dimensional mechanisms. The steady state at heat exchange surface temperature is commonly reached within (4 to 5) hours. The voltage and current were recorded when reaching steady state, in order to calculate the power supplied. The temperatures over the heat exchange surface were recorded and for a small equal specified distances to the Z-axis perpendicular to each point of the measurement grid by the specified thermocouple sensing till reaching the space or ambient temperature in order to calculate the thermal boundary layer thickness (δ) until the difference between measured temperature and the ambient temperature was approximately (θ=0.02). The temperature distribution was measure at different ranges of Rayleigh number as shown in Table (3).

To calculate the local heat transfer coefficient by natural convection, a thermal balance was done as follows:

$$-k_f \left.\frac{dT}{dz}\right|_{z=0} = h(T_w - T_\infty) \qquad (1)$$

Rearranging equation (1), the local heat transfer coefficient on the heat exchange surface is obtained as follows:

$$h = \frac{-k_f \left.\frac{dT}{dz}\right|_{z=0}}{(T_w - T_\infty)} \qquad (2)$$

By integrating equation (2) along the plate area, the average heat transfer coefficient has been calculated as follows:

$$\overline{h} = \frac{1}{A}\int_A h\,.dA \qquad (3)$$

The Local Nusselt number has been calculated from the following equation:

$$Nu_{L_o} = \frac{h.L_o}{k_f} \qquad (4)$$

Substituting equation (2) into equation (4) yields:

$$Nu_{L_o} = \frac{-L_o \left.\frac{dT}{dz}\right|_{z=o}}{(T_w - T_\infty)} \qquad (5)$$

$$Z = \frac{z}{L_o} \qquad (6)$$

$$\theta = \frac{T - T_\infty}{T_w - T_\infty} \qquad (7)$$

$$Nu_{L_o} = -\left.\frac{d\theta}{dZ}\right|_{z=o} \qquad (8)$$

So the average Nusselt number can be calculated by integrating local Nusselt number over the heat exchange surface as follows:

$$\overline{Nu}_{L_o} = \frac{1}{A}\int_0^{L_o}\int_0^{L_o} \left.\frac{d\theta}{dZ}\right|_{Z=0} .dx\,.dy \qquad (9)$$

The thermal energy transferred by radiation can be calculated from the following equation:

$$Q_{Radiation} = F * \sigma * \varepsilon * A * (T_w^{\,4} - T_a^{\,4}) \qquad (10)$$

RESULT AND DISCUSSION

Temperature Distribution **:-** Figures (3) and (4-a-b) show the dimensionless

temperatures distribution at symmetry axes (X-axis and Y-axis), at the planes (Z-X and Z-Y), above the surface of square plate and circular perforated surface specimens with and without plug for inclination with horizontal ($\Phi=0^o,45^o,90^o,135^o$, and 180^o), for ($Gr_{Lo}=1.576x10^6$, $3.546x10^6$, $5.083x10^6$, and $6.292x10^6$). Temperature gradient in the upward heating state is lower than the case of downward heating. The adiabatic plug prevents the additional flow, that results decrease in the temperature gradient leads to decrease the quantity of the heat transferred. Generally for all inclination angles (Φ), increasing heating level, (increasing Grashof number (Gr_{Lo})) and perforation ratio (m) leads to increase the temperature gradient for the specimens.

Thermal Boundary Layer Thickness (δ):- Figures (5) and (6-a-b) depict change of thermal boundary layer thickness above the surface of square plate and circular perforated surface specimens with and without plug above surface specimens in the (Z-Y) plane, for inclination angles from horizon ($\Phi=0^o,45^o,90^o,135^o$, and 180^o), at heating levels ($1.576x10^6\leq Gr_{Lo}\leq 6.292x10^6$). In general, thickness of thermal boundary layer decreases with increasing (Gr_{Lo}), and perforation ratio (m) for all inclination angles. It is observed that the maximum thickness of thermal boundary layer is at the center and falls gradually toward the edges. This is attributed to the fluid molecules density which is greater above the edges compared with density of fluid molecules density above the center, which possesses the maximum temperature at the surface. This leads to raise the lower density hot molecules above the center at higher speed causing pressure rarefaction, then the adjacent molecules of higher density move from the outer edges in a horizontal moving to replace them. The flow at the edges is parallel to the surface and accelerates toward the center near to it, at which the fluid moves upwards in the shape of a plume, called thermal separation region at center, thermal separation occurs at center and the quantity of heat transfer is minimum, while it is maximum at the edges. The fluid rise near the specimen center results for making thermal boundary layer it is maximum at the center in the horizontal position of specimen ($\Phi=0^o$), it is seen that the boundary layer thickness increases as compared with perforated specimens without plug, while the rate of heat transfer is reduced as a result of reduction of temperature gradient over perforated specimens surface in presence of plug (with no additional flow). In general thickness of thermal boundary layer decreases when (Gr_{Lo}) and perforation ratio increase for all inclination angles with the horizontal ($\Phi=0^o,45^o,90^o,135^o$, and 180^o), at four surface heating levels ($1.576x10^6\leq Gr_{Lo}\leq 6.292x10^6$).

Effect Of Inclination Angle On The Average Nusselt Number:- Figure (7-a-b) show the effect of inclination angle on the ($\overline{Nu}_{Lo}$) for the square specimen and circular perforated specimen with and without plug for inclination angles with the horizontal ($\Phi=0^o,45^o,90^o,135^o$, and 180^o) and for four surface heating levels ($1.576x10^6\leq Gr_{Lo}\leq 6.292x10^6$). It is observed that, increases of the ($\overline{Nu}_{Lo}$) in the case of heating upward with increasing inclination angle from ($\Phi=0^o$) reaching the vertical position of specimens ($\Phi=90^o$), where is the maximum value of the ($\overline{Nu}_{Lo}$).With increasing inclination angle of downward heating reaching the horizontal position ($\Phi=180^o$) the value of the ($\overline{Nu}_{Lo}$) is gradual decrease. Also, there is an increase in values of ($\overline{Nu}_{Lo}$) with increasing (Gr_{Lo}) and perforation ratio, while decreasing values of ($\overline{Nu}_{Lo}$) for perforated specimens with plug compared to those without plug due to lower temperature gradient above the perforated specimens with plug.

Effect Of Perforation Ratio On The Average Nusselt Number:- Figure (8-a-b) display the effect of perforation ratio on ($\overline{Nu}_{Lo}$) for the square specimen and circular perforated specimens with and without plug for inclination angles with the horizontal ($\Phi=0^o,45^o,90^o,135^o$, and 180^o), at surface heating levels ($1.576x10^6\leq Gr_{Lo}\leq 6.292x10^6$). It is noticed an increases in the value of ($\overline{Nu}_{Lo}$) with increasing perforation ratio, but the increase for circular perforated specimens

without plug is greater than for perforated specimens with plug, because with hole the thermal separation region can be removed, which is formed at the centre of square specimen and gets nearer to the flow of boundary layer at the specimen outer edges, which increases ($\overline{Nu}_{Lo}$).

Mathematical Correlation Between The Average Nusselt Number And Rayleigh Number:- Figure (9-a-b) for the square plate and circular perforated specimens with and without plug show a relationship, for upward and downward heating situation according to the following equation :

$$\overline{Nu}_{L_o} = C_1 (Ra.\sin\Phi)^{0.25} \quad \ldots\ldots(11)$$

It is also observed the values of the constant (C_1) for perforated specimens without plug is more than for the perforated specimens with plug.

Figures (10) and (11) show the effect of perforation ratio in correlation between ($\overline{Nu}_{Lo}$) and (Ra_{Lo}) for perforated specimens with and without plug in the upward and downward heating situations for different inclination angles in accordance with the following equation:

$$\overline{Nu}_{L_o} = (C_2 + C_3 \times m)(Ra.\sin\Phi)^{0.25} \quad \ldots\ldots (10)$$

The values of constants (C_2) and (C_3) in the upward heating case are lower than those in the downward heating case for the perforated specimens with and without plug.

Average Of Total Dimensionless Heat Transfer:- Figure (12-a-b) display the effect of perforation ratio(m) on average dimensionless heat transfer at Grashof number (Gr_{Lo}=1.576x10^6,3.546x10^6,5.083x10^6 and 6.292x10^6) for the square specimen and perforated specimens with and without plug. It is observed that the maximum heat transfer quantity is at perforation ratio (m=0.1), and gradually decreases with increasing perforation ratio (m=0.24 and 0.5), despite the increase in ($\overline{Nu}_{Lo}$), due to the decrease in the area of heat exchange, which leads to decrease in the rate of heat transfer. It is also observed the total heat transfer quantity to the perforated plates with plug is lower than that transfer to the perforated plates without plug, by (6.477%) for all perforation ratios due to decreasing ($\overline{Nu}_{Lo}$) for perforated plates with plug from that for perforated plates without plug.

Choice Of Suitable Hole Shape:- To investigate the perforated shape, and to determine the effect of most suitable hole shape on heat loss, a comparison has been done between quantity of heat transferred in the case of circular hole in present work with square hole as cited by [Ali, 2007] for the ratios of perforation are (m=0.1,0.16,0.24, and 0.36) for upward heating ($0^o<\Phi\leq 90^o$) and downward heating ($90^o\leq\Phi<180^o$), at four heating levels, as shown in Figure (13-a-b). It is found that heat transferred in the case of circular hole is greater than the heat quantity in the case of square hole for the same perforation ratios. It founded there is no effect of square hole edges "corners" which represented stagnation flow region[AL-Arabi and EL-Riedy, 1976], this led to thermal loss in case of circular hole is greater than in case of square hole.

Comparison Of Present Results With Previously Published Results:- There is agreement between results of present work for values of ($\overline{Nu}_{Lo}$) for horizontal square plate with its heated surface downward are shown in Figure (14) and for vertical position in Figure (15). And previous numerically published work by [Abd, 2007], and experimentally by [Ali, 2007] for horizontal square plates with their heated surface downwards, and in vertical position, also compared with previous numerical results for horizontal disc with heated surface downwards, and for heating in the vertical position with those by [Hassan, 2003]. Values of ($\overline{Nu}_{Lo}$) for inclined perforation square plate, with circular perforation, at perforation ratio (m=0.5) for both heating upward, shown in Figure (16) and heating downward shown in Figure (17) of present work with previous numerical work by [Abd, 2007], for an inclined square plate perforated with circular hole of perforation ratio (0.6), and with previous experimental work [Ali, 2007], for

an inclined square plate, perforated with square hole at perforation ratio (0.36) for upward and downward heating. There is good agreement in values of ($\overline{Nu}_{Lo}$) with results reported by [Abd, 2007], and the value of ($\overline{Nu}_{Lo}$) shows an increase, from the experimental results of [Ali, 2007], by (16.21%) for heating upwards, and by (18.74%) for heating downwards.

Conclusions:- The results show that for square specimen and specimens with circular hole without plug

1- The minimum temperature gradient and maximum thermal boundary layer thickness (δ) is above the centre of the square specimen in the horizontal position heated face upward ($\Phi=0^o$), while the gradient increases and thermal boundary layer thickness (δ) decreases when specimens are perforated.

2- The value of local Nusselt number (Nu_{Lo}) in the upward heating is less than in the downward heating, this leads to increase the quantity of heat transfer in the downward heating than in the upward heating. The maximum value of (Nu_{Lo}) is at the lower edge of inclined specimens in ($\Phi=90^o$).

3- Maximum value for the ($\overline{Nu}_{Lo}$) is in the vertical position ($\Phi=90^o$), and minimum value is in both horizontal position ($\Phi=0^o,180^o$). The ($\overline{Nu}_{Lo}$) increases with increasing perforation ratio and heating level to reach its maximum value at perforation ratio (m=0.5) and ($Gr_{Lo}=6.292x10^6$) in ($\Phi=90^o$).

4- Maximum heat transfer quantity is at perforation area ratio (m=0.1), and maximum heat transfer rate for square and perforated specimens is in the vertical position ($\Phi=90^o$) at all heating levels .

5- The realization of an empirical correlation for ($\overline{Nu}_{Lo}$) with term (Ra.sinΦ) and perforation ratio for square specimens having circular perforation with heated surface upwards without plug
{$\overline{Nu}_{Lo}=(0.599+0.407Xm)(Ra.\sin\Phi)^{0.25}$}, and its heated surface downwards {$\overline{Nu}_{Lo}=(0.634+0.333Xm)(Ra.\sin\Phi)^{0.25}$}.

6- The rate of heat transfer for circular hole is greater than for square hole for the same perforation ratio .

The results show for circular perforated specimens with plug

1- Decrease in temperature gradient and increase in the thermal boundary layer thickness (δ) occur in the perforated specimens with plug.

2- The values of local Nusselt number and quantity of heat transfer are lower than those without the plug.

3- The average Nusselt number for perforated specimens with plug is lower than without.

4- The quantity of heat transfer for perforated specimens with plug, is lower than that without plug by (6.477%) for all perforation ratios. The maximum values of the heat transfer is at the vertical position ($\Phi=90^o$) for all heating levels.

5- In order to formulate an empirical correlation for average Nusselt number ($\overline{Nu}_{Lo}$) with the expression (Ra.sinΦ) and perforation ratio for square specimens having circular hole with its heated surface upwards with plug {$\overline{Nu}_{Lo}=(0.544+0.287Xm)(Ra.\sin\Phi)^{0.25}$}, and its heated surface downwards {$\overline{Nu}_{Lo}=(0.566+0.305Xm)(Ra.\sin\Phi)^{0.25}$}.

References

Abd Y. H. 2007
"Numerical Study For A Three Dimensional Laminar Natural Convection Heat Transfer From An Isothermal Heated Horizontal And Inclined Square Plate And With A Circle Hole".
Journal of Engineering Vol. 13, No.2,

AL-Arabi M. & EL-Riedy M. K. 1976
"Natural Convection Heat Transfer From Isothermal Horizontal Plates of Different Shapes".
Int. J.Heat & Mass Transfer . Vol. 19 , PP. 1399-1404.

Ali Th. H. 2007
"Experimental Study For A Three Dimensional Laminar Natural Convection Heat Transfer From An Isothermal Heated Square Plate".
M. Sc. Thesis Univ. Technology.

Aziz R. N. 2002
"Instructional System To Study Free Convection Heat Transfer from Isothermal Horizontal Square Flat Surfaces ".
M. Sc. Thesis Univ. Technology

Hassan A. K. 2003
"Prediction of Three Dimensional Natural Convection from Heated Disks and Rings at Constant Temperature ".
J. Eng. & Technology. Vol. 22, No.5, PP. 229

Robinson S. B. & Liburdy J. A. 1987
"Prediction of The Natural Convection Heat Transfer From A Horizontal Heated Disk".
Transactions of the ASME . Vol. 109 , PP. 906-911-248

Pera Luciano & Gebhart Benjamin 1973
"Natural Convection Boundary Layer Flow Over Horizontal And Slightly Inclined Surfaces".
Int.J. Heat & Mass Transfer . Vol. 16 , PP. 1131-1145.

Mustafa A. W. 2001
"Numerical and Experimental Study of Natural Convection Heat Transfer from Isothermal Horizontal Disks and Rings".
M. Sc. Thesis Univ. Technology

Sahraoui M. , Kaviany M. & Marshall H. 1990
"Natural Convection From Horizontal Disks And Rings " .
Transactions of the Asme . Vol. 112 , PP. 110-116

List Of Symbols

Nomenclature

Symbol	Definition	Unit
A	Total surface area	m^2
$C_1, C_2, C_3,$	Empirical constants of average Nusselt number with Rayleigh number correlation	------
D_o	Disc diameter	m
F	Shape factor	------
$\overline{h}$	Average heat transfer coefficient	$W/m^2.{}^oC$
h	Local heat transfer coefficient	$W/m^2.{}^oC$
k_f	Fluid Thermal conductivity at film temperature	$W/m.{}^oC$
L_i	Inner length for the square hole	m
L_o	Length of square side	m
L_p	Length of rectangular surface	m
m	Ratio of hole area to square plate area	------
q	Convective heat transfer rate calculated from local measurement method	W
Q	Dimensionless heat transfer rate by convection	------
$Q_{convcetion}$	Convection heat transfer rate calculated from energy balance method	W
$Q_{radiation}$	Radiation heat transfer rate from specimen surface	W
R^2	Correlation coefficient	------
T	Temperature	^oC
T_∞	Ambient (atmospheric) temperature	^oC
T_w	Heated surface temperature	^oC
x,y,z	Normal coordinates	m

Dimensionless Group

$Gr_{Do} = g\beta(T_w - T_\infty)D_o{}^3/\upsilon^2$	Grashof number based on the outer diameter of disc or ring
$Gr_{Lo} = g\beta(T_w - T_\infty)L_o{}^3/\upsilon^2$	Grashof number based on the side length of square plate
$Nu_{Lo} = h.L_o/k_f$	Local Nusselt number based on the side length of square plate
$\overline{Nu}_{Lo} = \overline{h}.L_o/k_f$	Average Nusselt number based on the side length of square plate
$\overline{Nu}_{Do} = \overline{h}.D_o/k_f$	Average Nusselt number based on the outer diameter of disc or ring
$\overline{Nu}_{Lo} = \overline{h}.L_o/k_f$	Average Nusselt number based on the side length of square plate
$\overline{Nu}_{Lo-Li} = \overline{h}.(L_o - Li)/k_f$	Average Nusselt number based on the difference between the length of square plate and hole length
$\overline{Nu}_{Lp} = \overline{h}.L_p/k_f$	Average Nusselt number based on the side length of rectangular plate
$\Pr = \upsilon/\alpha$	Prandtl Number
$Ra_{Do} = Gr_{Do}\cdot P_r$	Rayleigh number based on outer diameter for disc or ring
$Ra_{Lo} = Gr_{Lo}\cdot P_r$	Rayleigh number based on the side length of square plate
$Ra_{Lp} = Gr_{Lp}\cdot P_r$	Rayleigh number based on the side length of rectangular plate

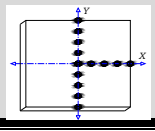
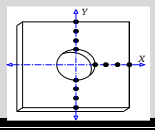
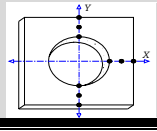
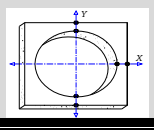
Greek Symbols

Φ	Angle of plate inclination from horizon	*degree*
σ	Stefan-Boltzman constant and it value 5.678×10^{-8}	W/m^2K^4
ε	Emissivity of heat exchange surface	------
θ	Dimensionless temperature	------
δ	Thickness of thermal boundary layer	*mm*

Table (1) the results of previous studies

Source	Type of Study	Plate Position	Geometric Figure	Characteristic Length	*Dimensionless Equation*	The Ranges
Pera & Gebhart (1973)	Experimental & Numerical	Horizontal & tilt 2o≤Φ≤6o	Rectangle	L_p	upface heated T_w=C $Nu_{Lp} = 0.394 Ra_{Lp}^{1/5} \Pr^{1/20}$ $Nu_{Lp} = 0.656 Ra_{Lp}^{1/5} \Pr^{1/20}$	$2.8x10^3 \le Ra_{Lp} \le 3x10^5$ Φ=0° $4.8x10^3 \le Ra_{Lp} \le 3.5x10^5$ 2°≤Φ≤6° at Pr = 0.72
AL-Arabi & EL-Riedy (1976)	Experimental	Horizontal	Square, Circular & Rectangle	L_o D_o L_p	upface heated $\overline{Nu}_{Lo,Do,Lp} = 0.70 Ra_{Lo,Do,Lp}^{1/4}$ Laminar flow region ---- $\overline{Nu}_{Lo,Do,Lp} = 0.155 Ra_{Lo,Do,Lp}^{1/3}$ Turbulent flow region	$2x10^5 < Ra_{Lo,Do,Lp} < 4x10^7$ ---- $4x10^5 < Ra_{Lo,Do,Lp}$
Robinson & Liburdy (1987)	Experimental & Numerical	Horizontal	disk	D_o	$\overline{Nu}_{Do} = 0.602 Ra_{Do}^{1/5}$	$7.7x10^4 \le Gr_{Do} \le 1.2x10^5$ $10^4 \le Gr_{Do} \le 10^6$ Pr=0.72
Sahraoui et al. (1990)	Experimental & Numerical	Horizontal	disks & rings with and without adiabatic core	D_o	upface heated $\overline{Nu}_{Do} = 0.561 Ra_{Do}^{1/5} \Pr^{0.085}$ ------ $\overline{Nu}_{Do} = 0.603 Ra_{Do}^{1/5} \Pr^{0.085}$	$10 \le Ra_{Do} \le 1.25x10^5$ $0.1 \le \Pr \le 10$
Mustafa (2001)	Experimental & Numerical	Horizontal	Disk & ring	D_o	upface heated $\overline{Nu}_{Do} = 0.95 Ra_{Do}^{0.192}$ ------ $\overline{Nu}_{Do} = (3r_2 + 0.95) Ra_{Do}^{0.192}$	$7x10^2 \le Ra_{Do} \le 7x10^6$ Pr=0.7 $r_2 = D_i / D_O$
Aziz (2002)	Experimental	Horizontal	square with and without square hole	L_o L_o-L_i	upface heated $\overline{Nu}_{Lo} = 0.73 Ra_{Lo}^{0.21}$ $\overline{Nu}_{Lo\text{-}Li} = 0.978 Ra_{Lo\text{-}Li}^{0.21}$	$10^6 < Ra_{Lo} < 4.5x10^6$ $4.18x10^5 < Ra_{Lo} < 1.73x10^6$ Pr=0.72
Abd (2007)	Numerical	Horizontal, vertical & tilt to the horizon	square with and without circular hole	L_o	upface heated $\overline{Nu}_{Lo} = 0.784 Ra_{Lo}^{1/5}$ $\overline{Nu}_{Lo} = (0.597 + 0.413\ r_1)(Ra_{Lo} \sin\Phi)^{0.25}$ ------ downface heated $\overline{Nu}_{Lo} = 0.78 Ra_{Lo}^{1/5}$ $\overline{Nu}_{Lo} = (0.604 + 0.423\ r_1)(Ra_{Lo} \sin\Phi)^{0.25}$	$7.2x10^2 \le Ra_{Lo} \le 3.6x10^4$ Pr = 0.72 $r_1 = a / Lo$
Ali (2007)	Experimental	Horizontal, vertical & tilt to the horizon	square with and without square hole	L_o	upface heated $\overline{Nu}_{Lo} = (0.584 + 0.222m)(Ra_{Lo} \sin\Phi)^{0.25}$ ------ downface heated $\overline{Nu}_{Lo} = (0.606 + 0.267m)(Ra_{Lo} \sin\Phi)^{0.25}$	$m = \frac{A_{hole}}{A_{square}}$ $10^6 \le Ra_{Lo} \le 3.96X10^6$

Table (2) Basic dimensions of the specimens used in the laboratory experiments

Specimens arrangement					
		First Specimen	***Second Specimen***	***Third Specimen***	***Fourth Specimen***
Type		Square plate	Square plate with circular hole	Square plate with circular hole	Square plate with circular hole
Dimen-sions	***Thickness***	10mm	10mm	10mm	10mm
	External side length	100mm	100mm	100mm	100mm
	circular hole diameter	0 mm	36mm	56 mm	80mm
Area ratio (m)		m=0.00	m=0.10	m=0.24	m=0.50

Table(3) Grashof number(Gr_{Lo}) and Rayleigh number(Ra_{Lo}) ranges of the experiments

T_w (°C)	40	60	80	100
T_{film} (K)	306.5	316.5	326.5	336.5
Gr_{Lo}	1.576×10^6	3.546×10^6	5.083×10^6	6.292×10^6
Ra_{Lo}	1.112×10^6	2.496×10^6	3.568×10^6	4.398×10^6

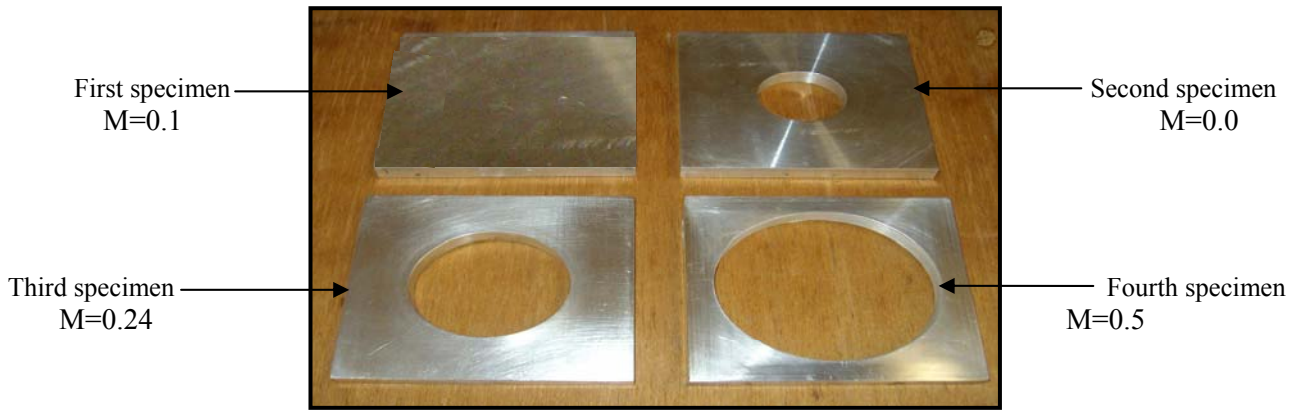
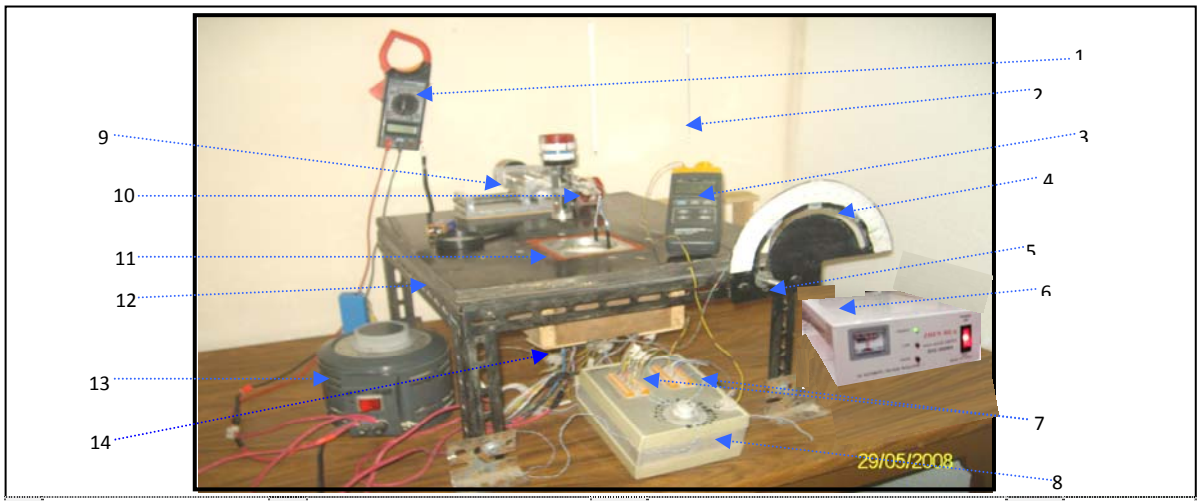


Figure (1) Specimens used in the experimental tests



1	Digital clamp meter	5	Screw & nut	9	3-dimensional movement mechanism	13	Variac
2	Mercury thermometer	6	Automatic voltage regulator	10	Holder	14	Wool box
3	Digital thermometer	7	Extension wires	11	Specimen		
4	Protractor	8	Selector switch	12	Extending surface		

Figure (2) Test rig with measurement devices

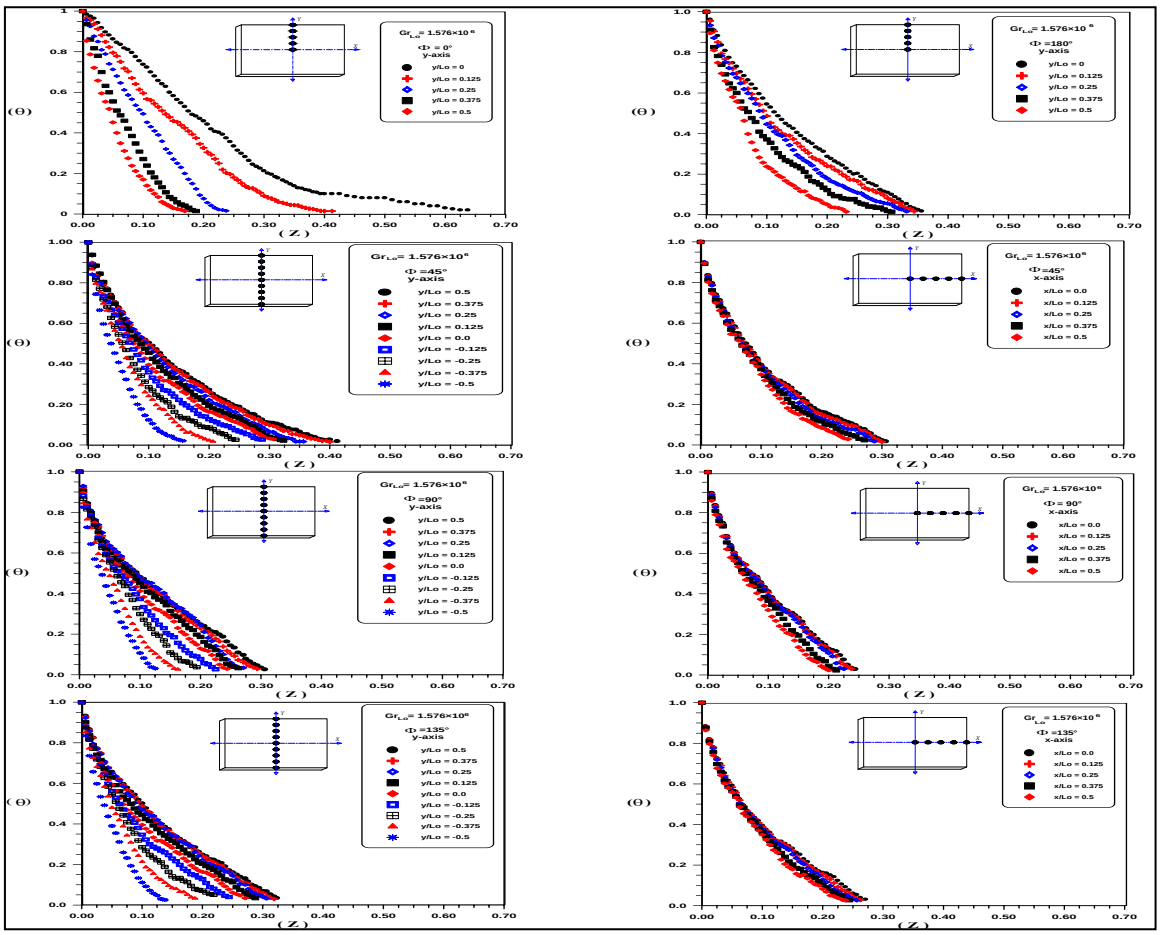
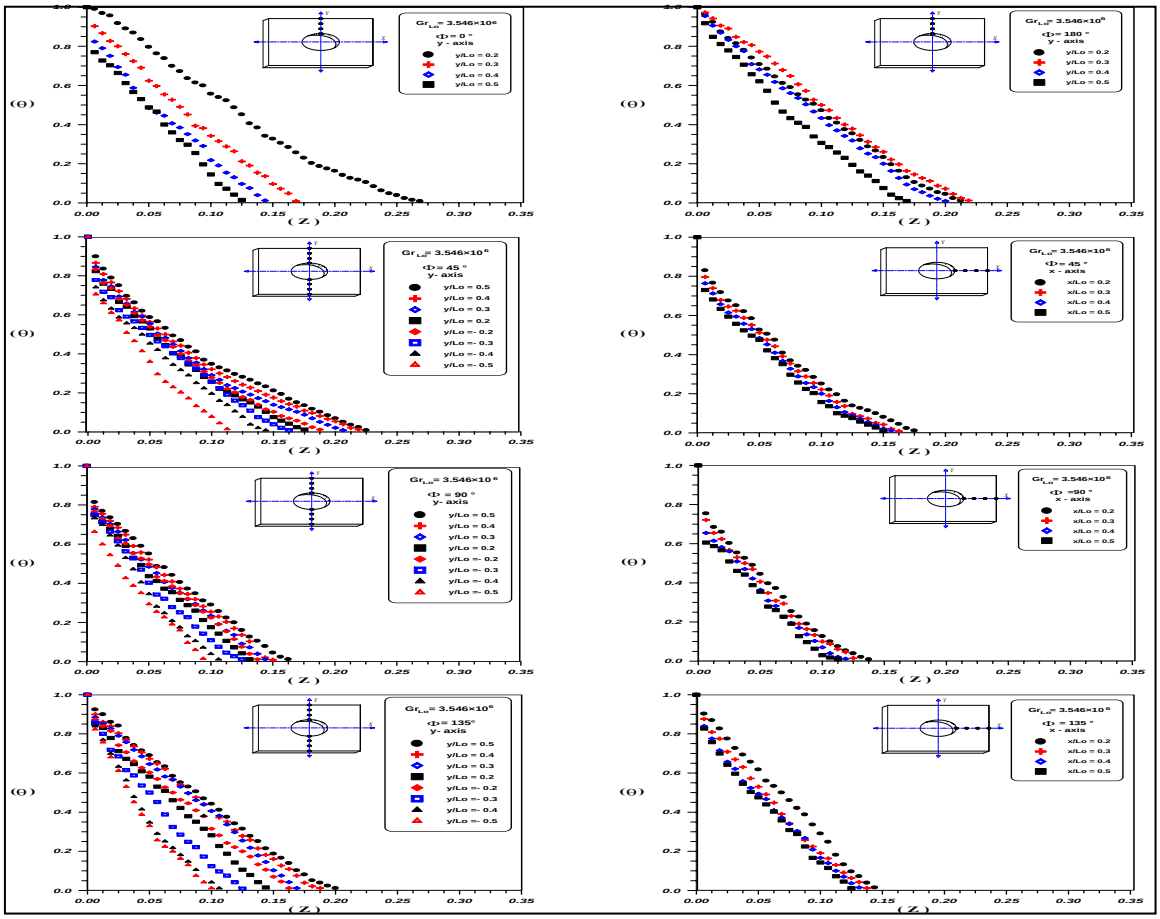


Figure (3)experimental temperature distribution over 1st specimen m=0.0 for Gr_{Lo}=1.576X10^6



Figure(4-a) experimental temperature distribution over 2ed specimen without plug m=0.1 for Gr_{Lo}=3.546X10^6

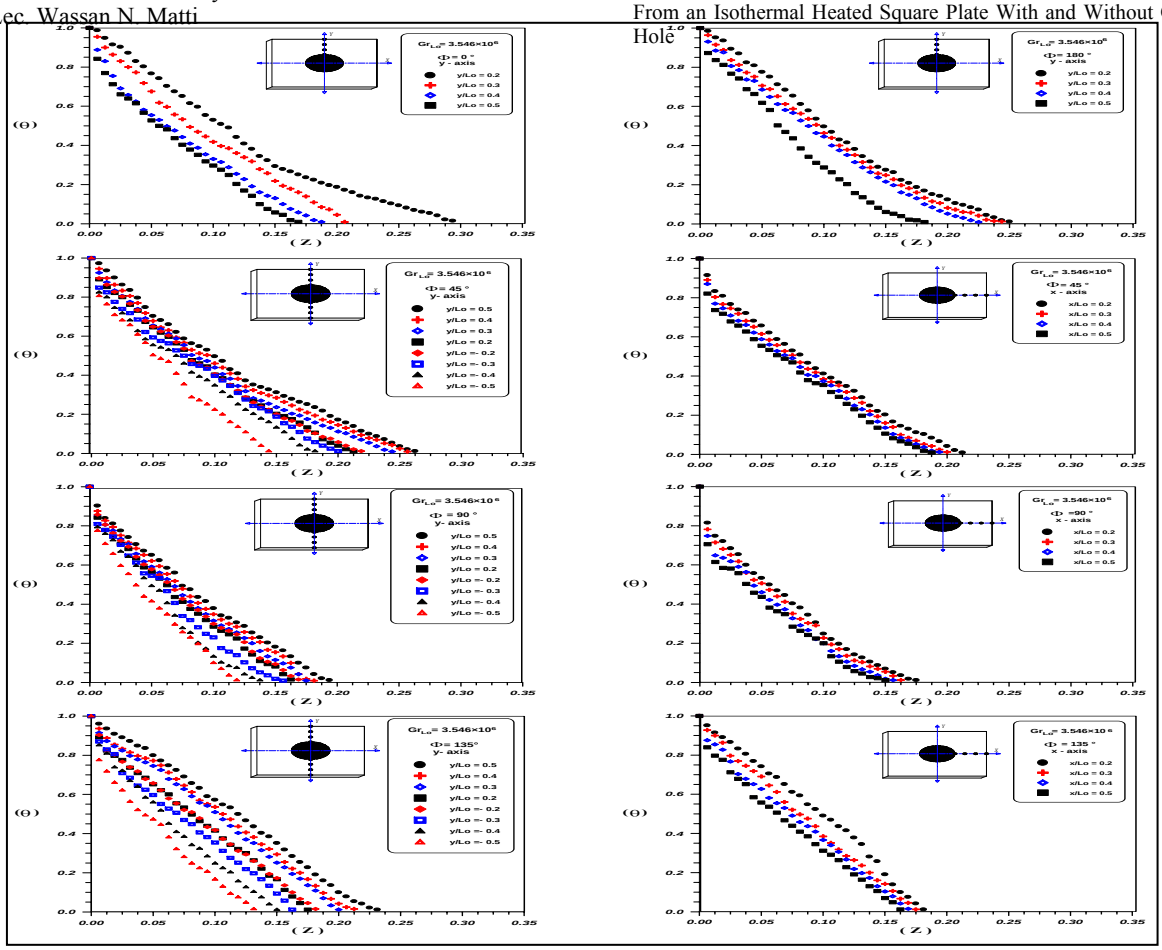
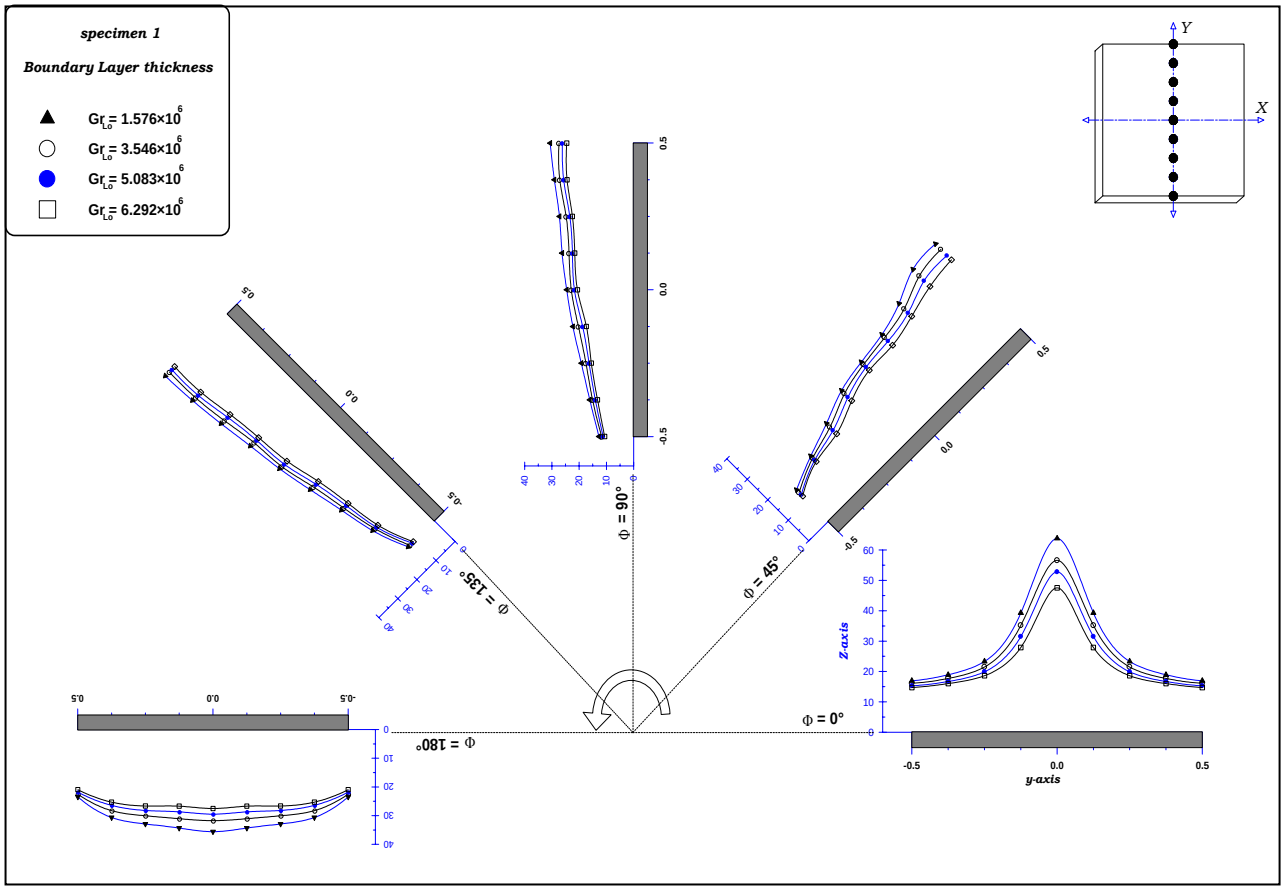
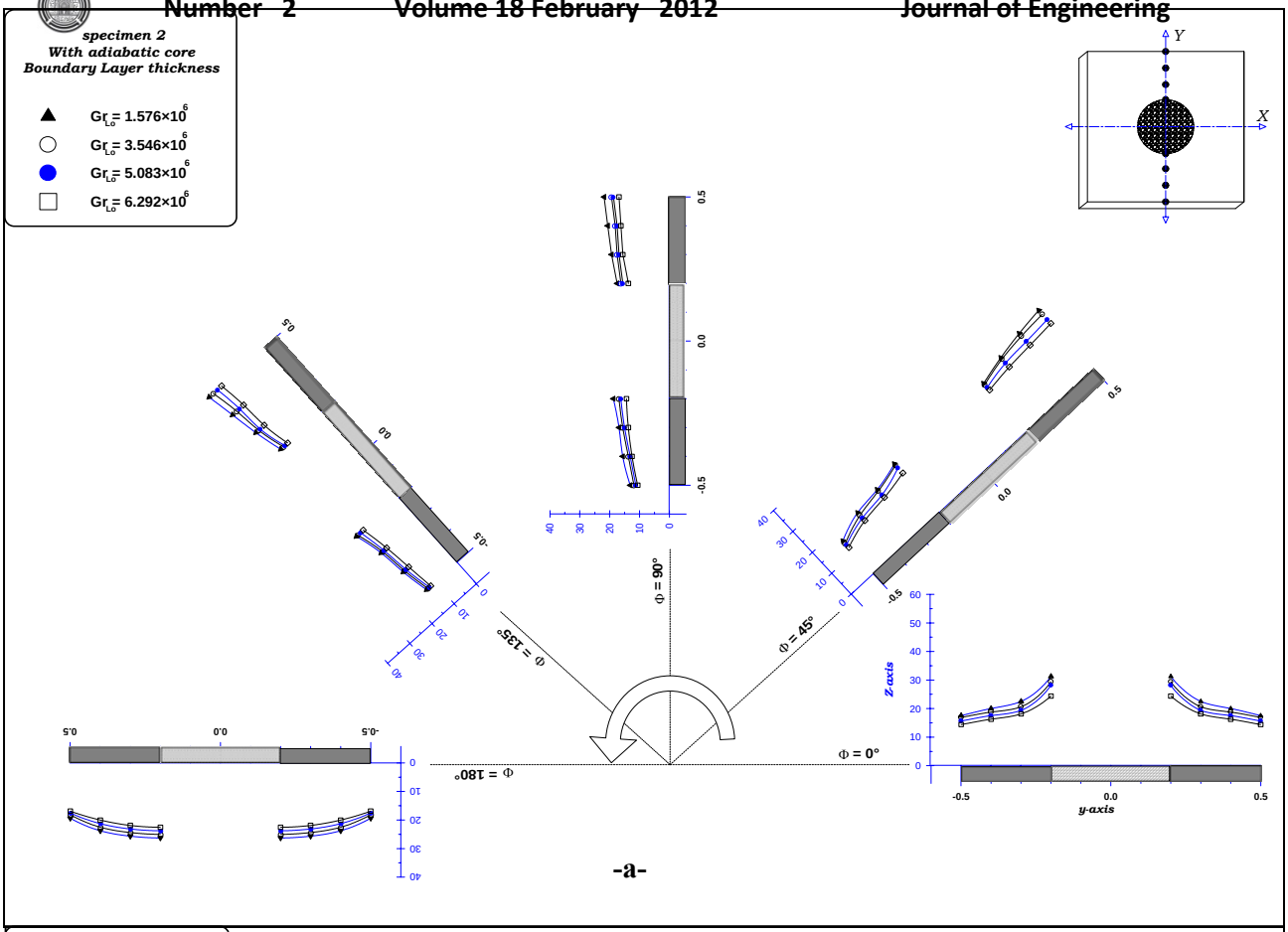


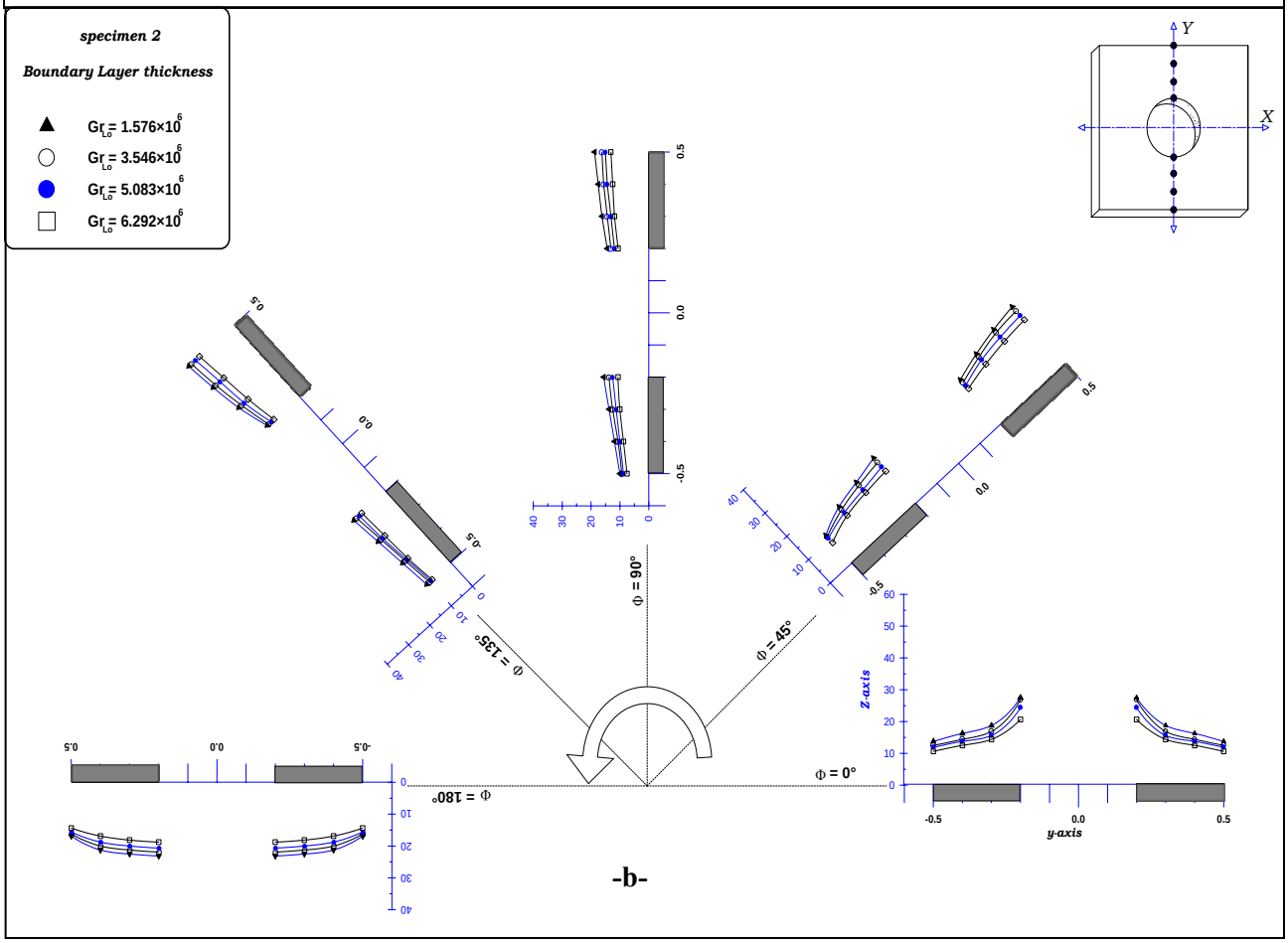
Figure (4-b) experimental temperature distribution over 2[ed] specimen with plug m=0.1for $Gr_{L_0}=3.546X10^6$



Figure(5) boundary layer thickness over 1[st] specimen surface m=0.0 for $(1.576x10^6 \leq Gr_{L_0} \leq 6.292x10^6)$



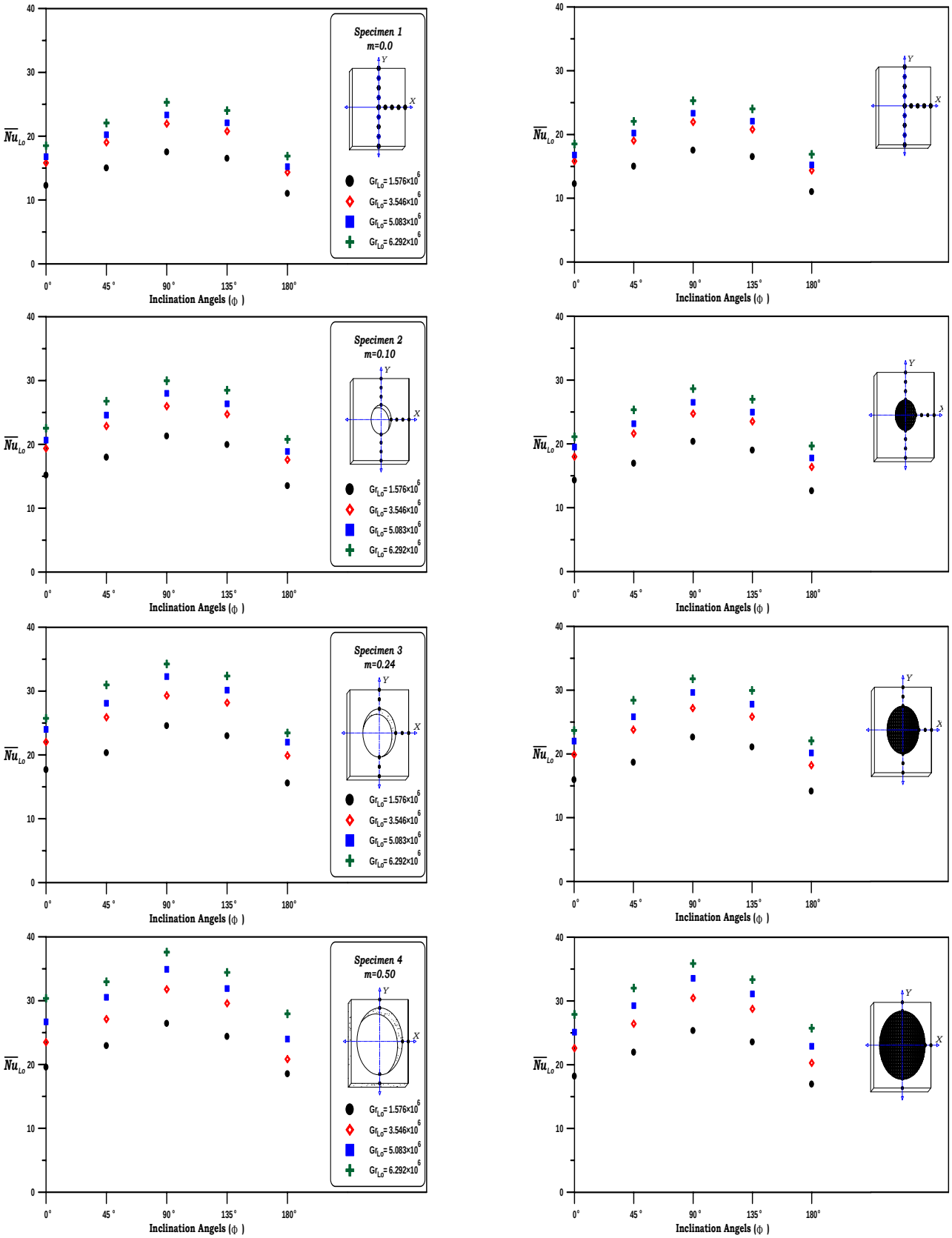
-a-



-b-

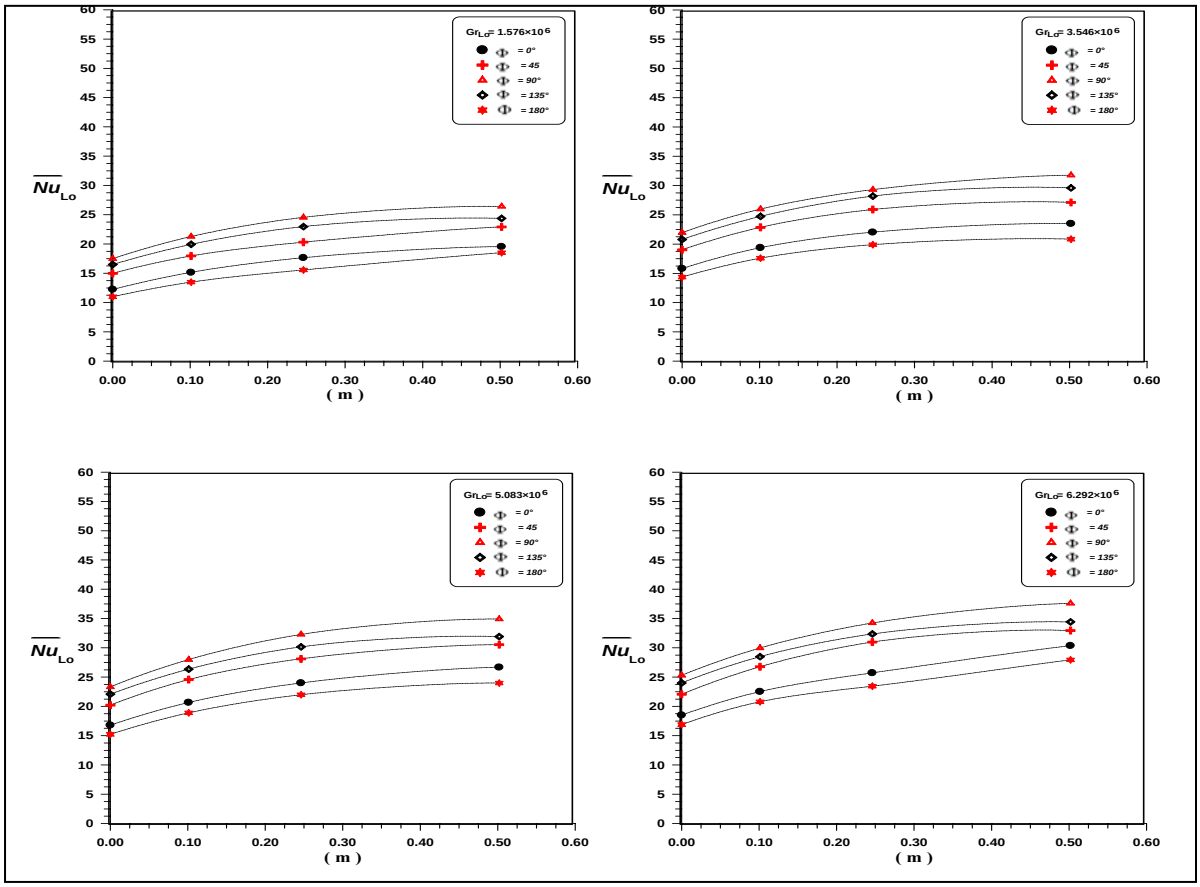
Figure(6) boundary layer thickness over 2[ed] specimen surface m=0.1 for ($1.576x10^6 \leq Gr_{Lo} \leq 6.292x10^6$)

-a- without plug (adiabatic core) for circular hole -b- with plug (adiabatic core) for circular hole

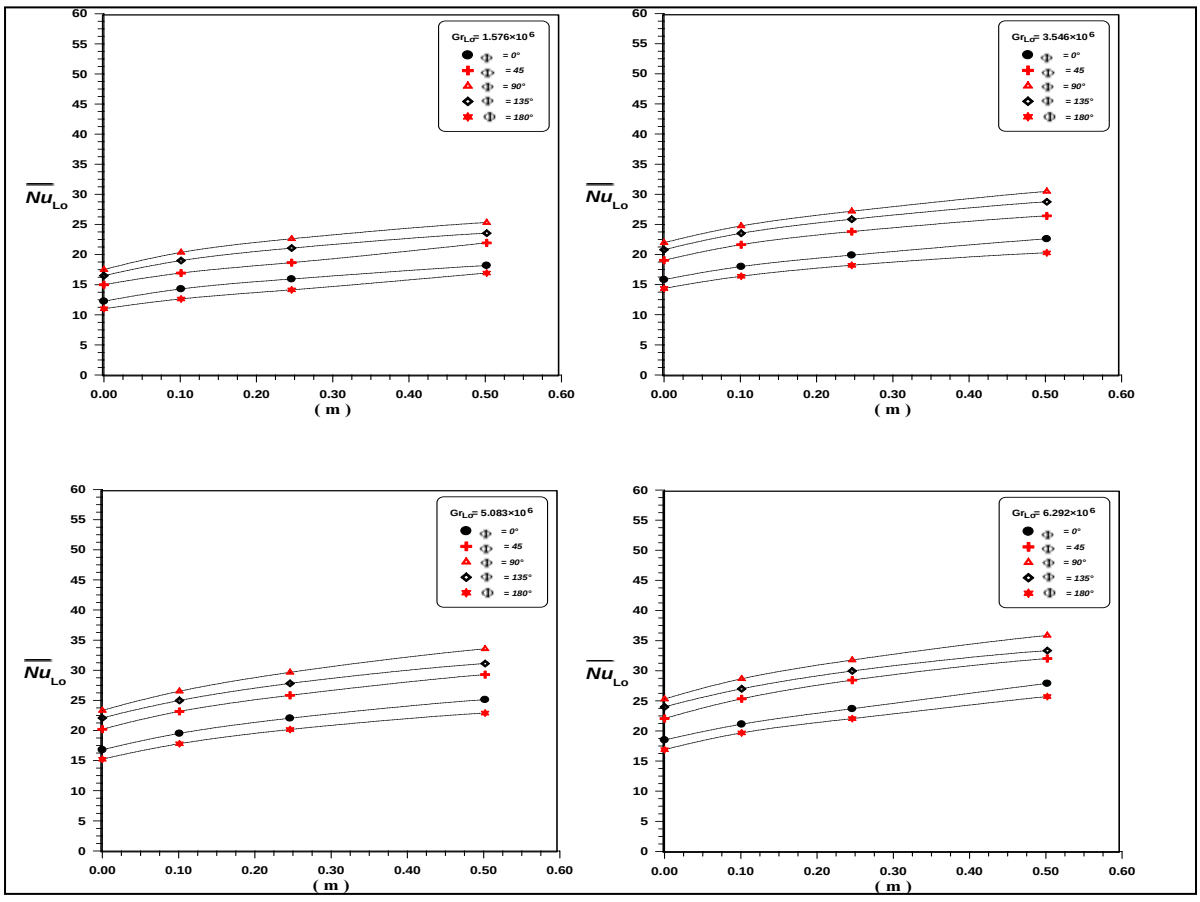


-a- -b-

Figure (7) the effect of inclination angle (Φ) from horizon on ($\overline{Nu}_{Lo}$)
-a- without plug (adiabatic core) for circular hole
-b- with plug (adiabatic core) for circular hole

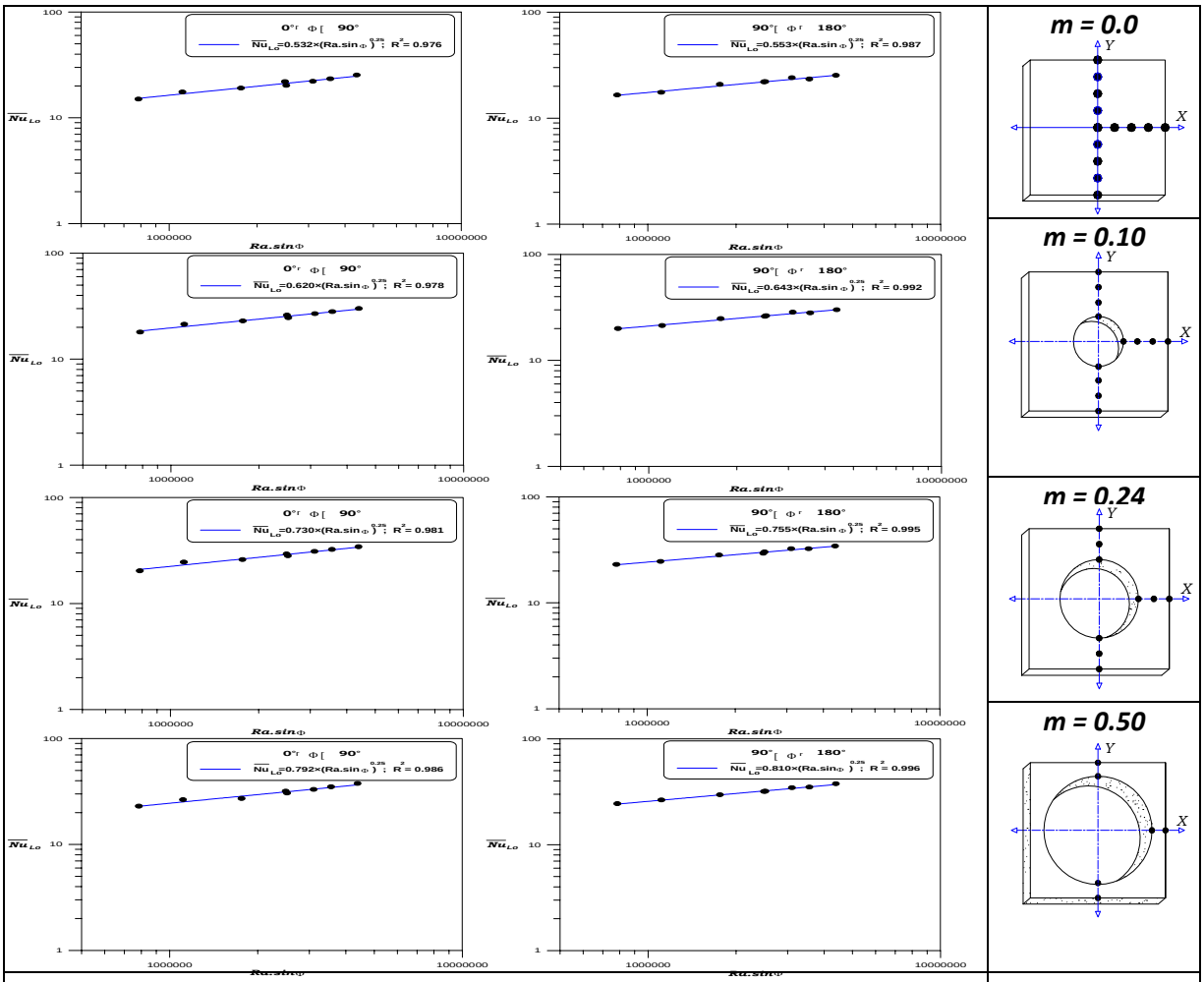


-a-

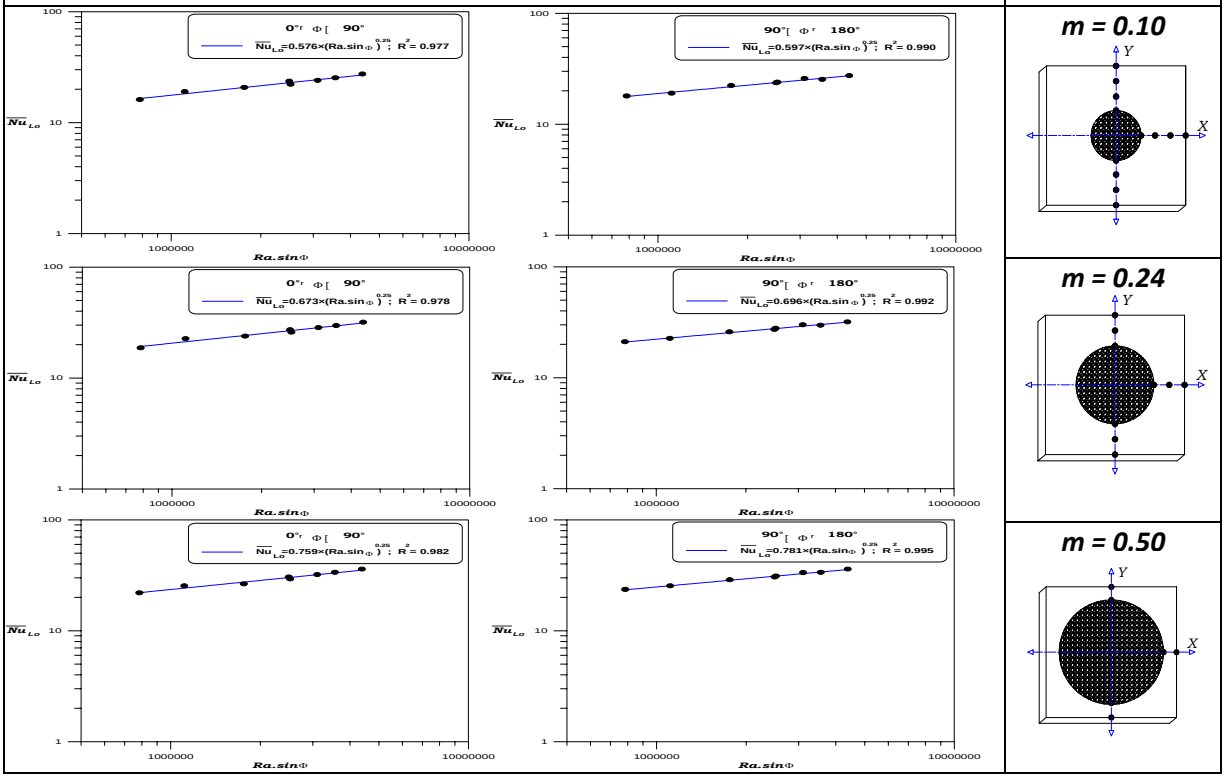


-b-

) for four heating levels $\overline{Nu}_{Lo}$ Figure (8) the effect of perforation ratio (m) on the (
-a- without plug (adiabatic core) for circular hole
-b- with plug (adiabatic core) for circular hole



-a-



-b-

Figure (9) correlation between ($\overline{Nu}_{Lo}$) & (Ra_{L0}) for specimens heating face upward & downward
-a- without plug (adiabatic core) for circular hole -b- with plug (adiabatic core) for circular hole

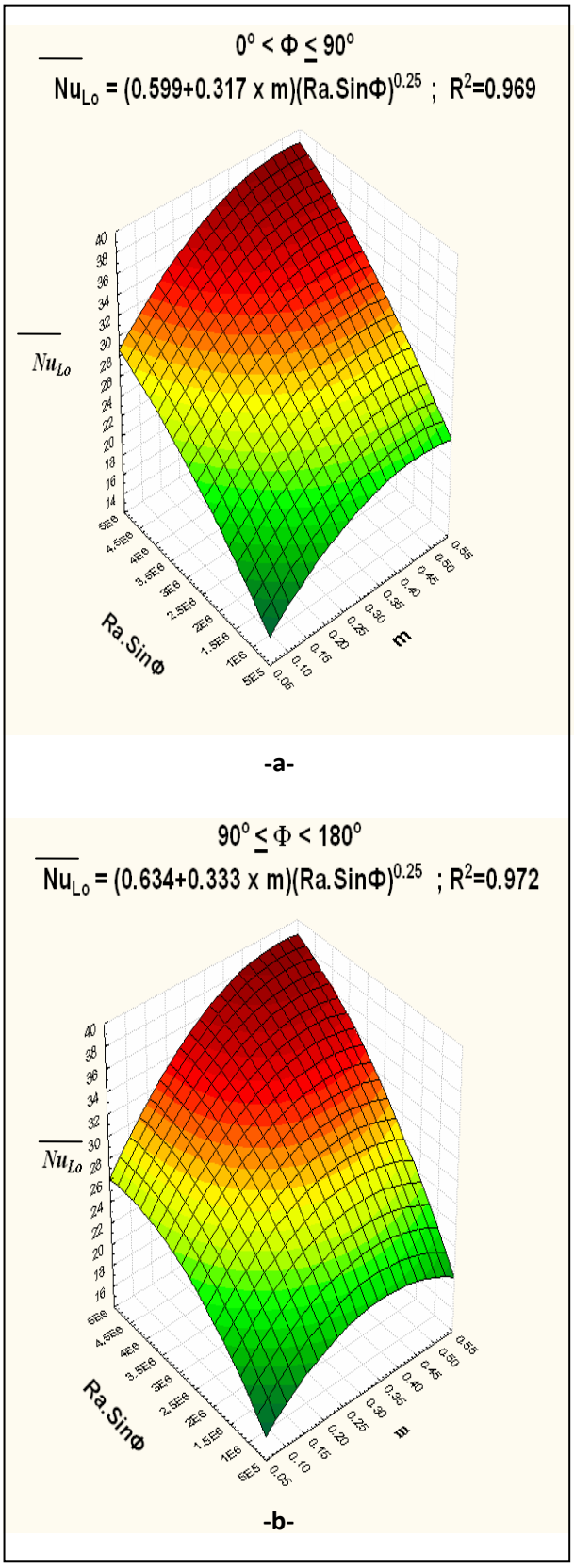


Figure (10) ($\overline{Nu}_{Lo}$) as a function of Ra sin(Φ) & perforation ratio (m) for specimens without plug (adiabatic core) for circular hole
-a- upface heated
-b- downface heated

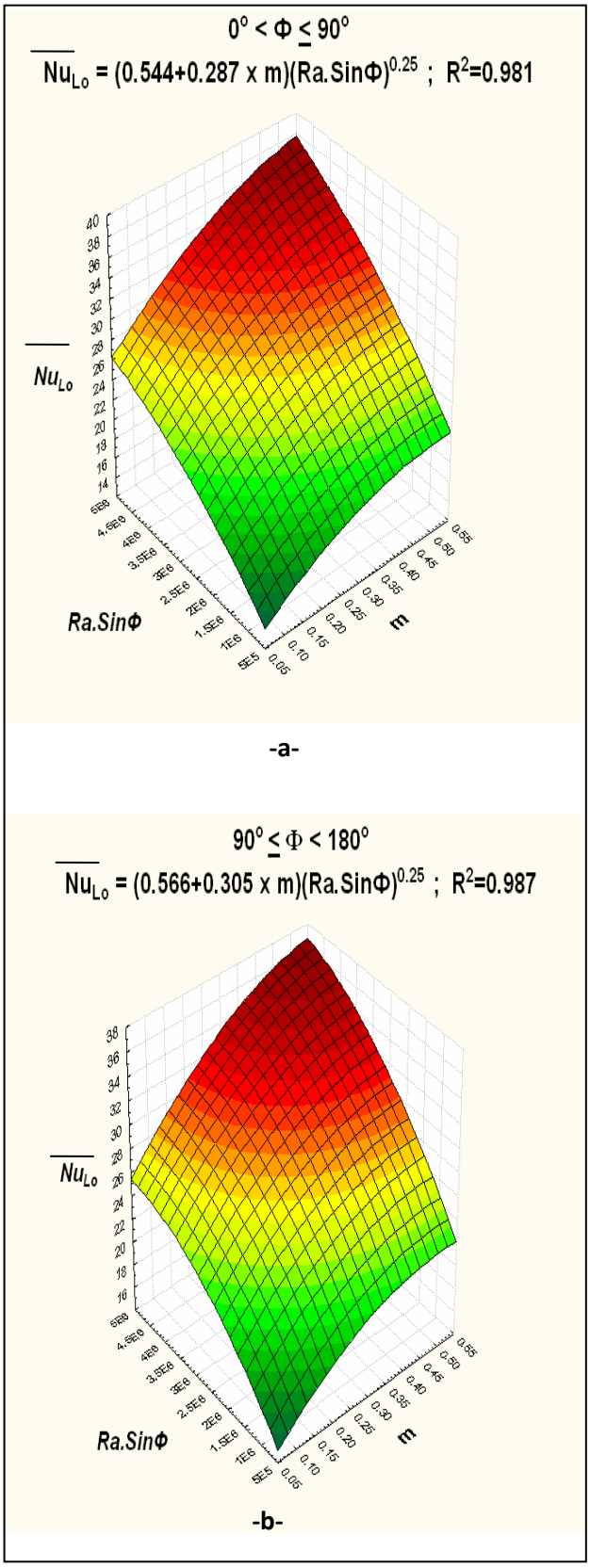


Figure (11) ($\overline{Nu}_{Lo}$) as a function of Ra sin(Φ) & perforation ratio (m) for specimens with plug (adiabatic core) for circular hole
-a- upface heated
-b- downface heated

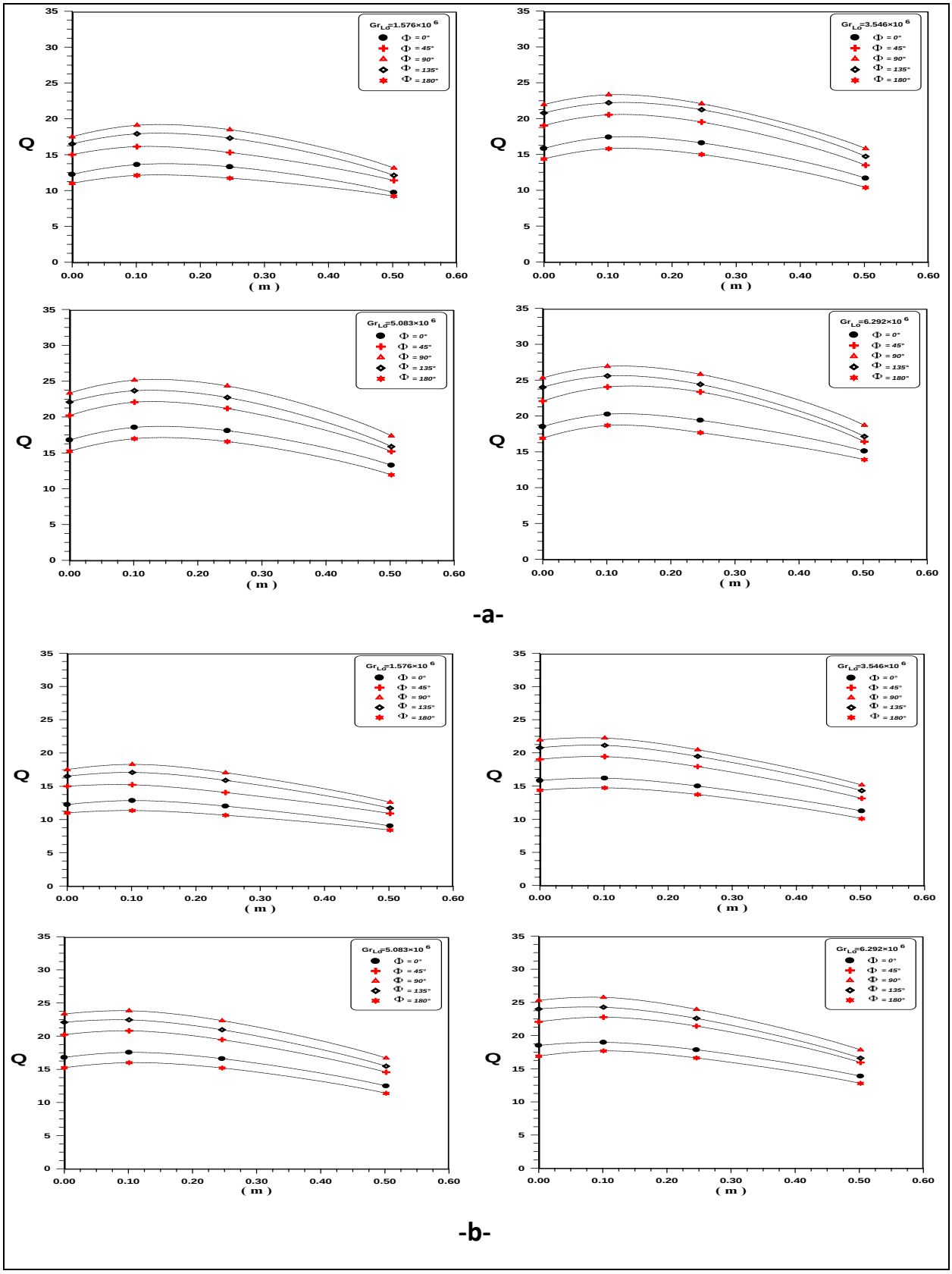


Figure (12) the effect of perforation ratio (m) on the dimensionless heat transfer rate for different heating levels
-a- without plug (adiabatic core) for circular hole
-b- with plug (adiabatic core) for circular hole

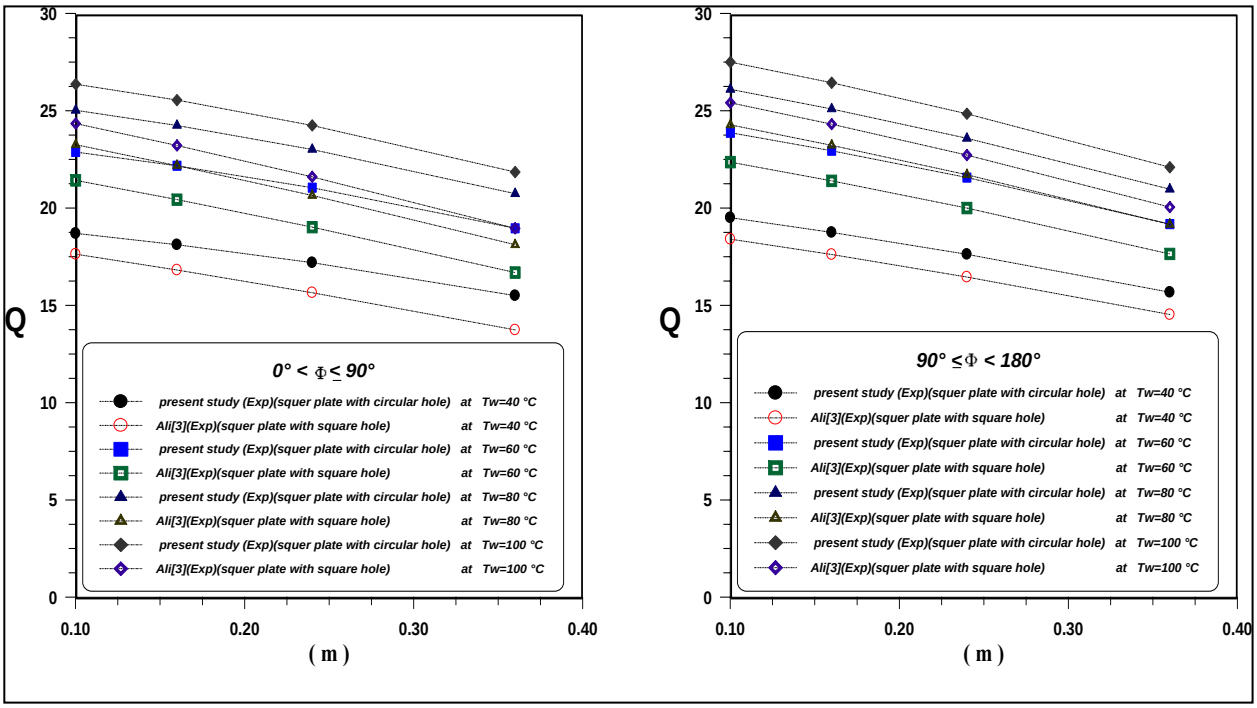
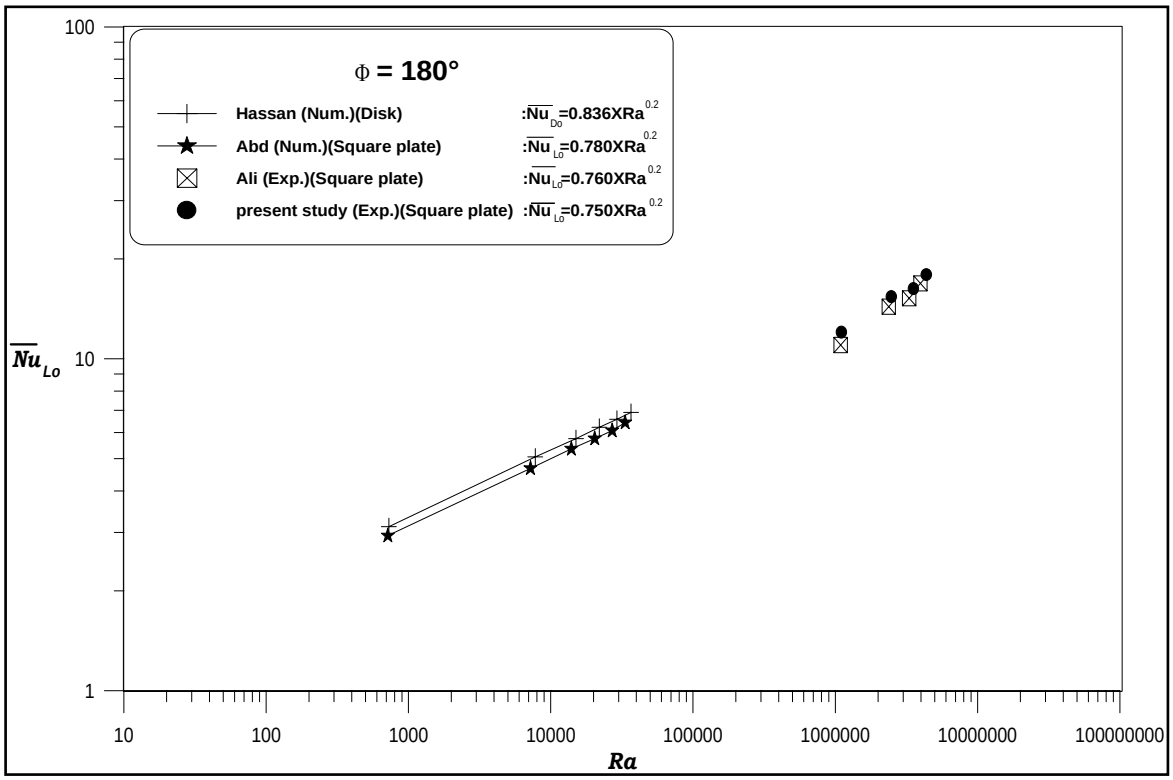
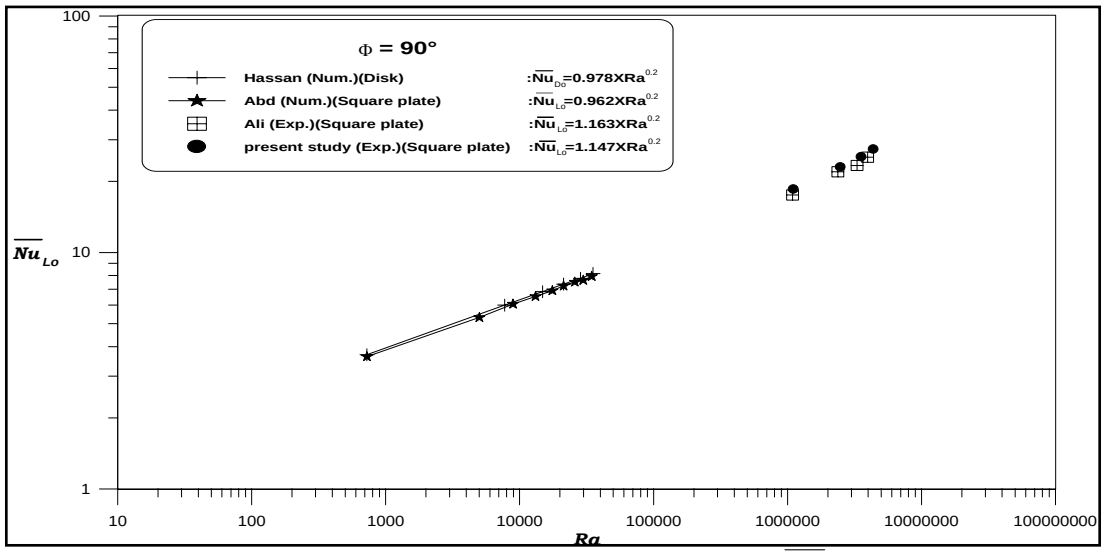


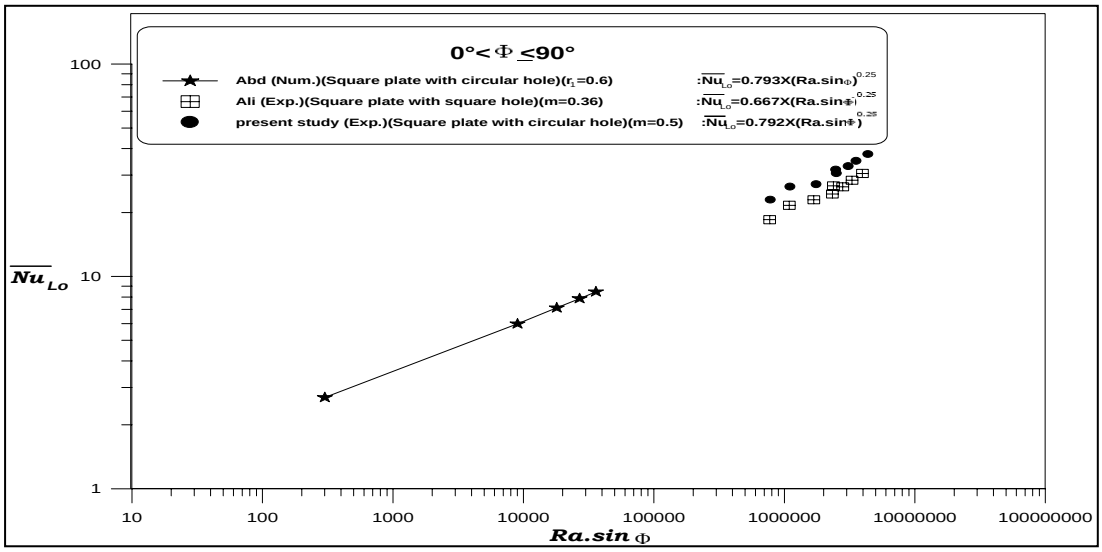
Figure (13) effect hole shape on the dimensionless heat transfer rate for different heating levels and fore perforation ratio (m=0.1,0.16,0.24,0.36)
a- upface heated b- downface heated



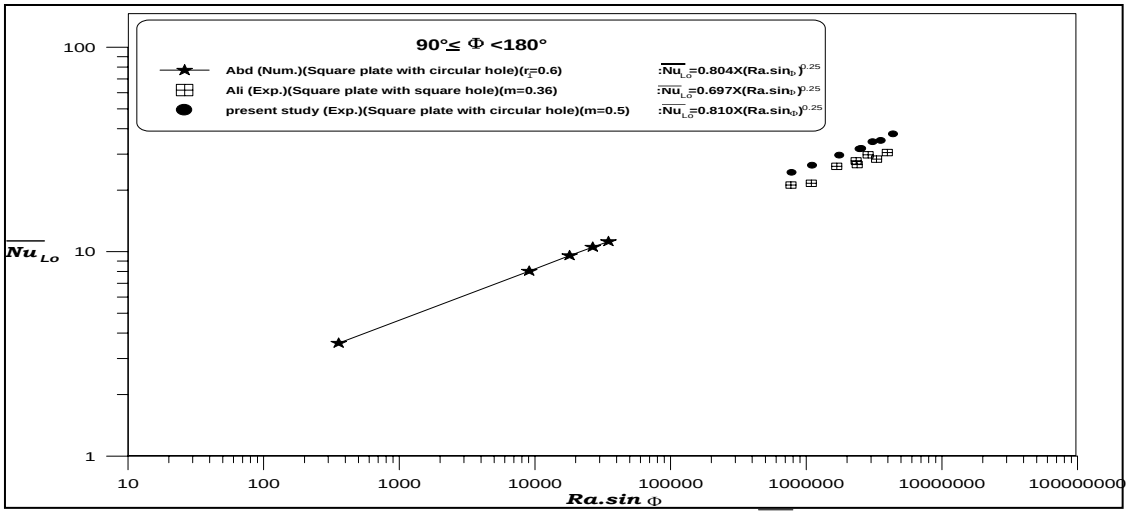
) number for present study horizontal square plate with $\overline{Nu}_{Lo}$ Figure (14) comparison (experimental & numerical previous studies for horizontal square plates &disks at downface heated



) number for present study at vertical position square plate $\overline{Nu}_{Lo}$ Figure (15) comparison (with experimental & numerical previous studies for square plates &disks at vertical position



) number for present study perforate square plate with $\overline{Nu}_{Lo}$ Figure (16) comparison (experimental & numerical previous studies for perforate square plates with circular, square hole & ring at upface heated



) number for present study perforate square plate with $\overline{Nu}_{Lo}$ Figure (17) comparison (experimental & numerical previous studies for perforate square plates with circular,squar hole & ring at downface heated